Carbohydrate Polymers 92 (2013) 662–667

Contents lists available at SciVerse ScienceDirect

Carbohydrate Polymers

journal homepage: www.elsevier.com/locate/carbpol

Dual stimuli-responsive *N*-phthaloylchitosan-*graft*-(poly(*N*-isopropylacrylamide)-*block*-poly(acrylic acid)) copolymer prepared via RAFT polymerization

Ke Zhang[a], Zhengke Wang[a,*], Youliang Li[a], Zhiqiang Jiang[a], Qiaoling Hu[a,*], Minying Liu[b,**], Qingxiang Zhao[b]

[a] *MOE Key Laboratory of Macromolecular Synthesis and Functionalization, Department of Polymer Science and Engineering, Zhejiang University, Hangzhou 310027, China*
[b] *School of Materials Science and Engineering, Zhengzhou University, Zhengzhou 450052, China*

ARTICLE INFO

Article history:
Received 14 June 2012
Received in revised form 1 September 2012
Accepted 3 September 2012
Available online 7 September 2012

Keywords:
Chitosan
RAFT
Stimuli–response
Graft modification
Micelle

ABSTRACT

In order to develop stimuli-responsive hydrogel, chitosan graft copolymer with chitosan back-bone and poly(*N*-isopropylacrylamide)-*block*-poly(acrylic acid) (PNIPAAm-*b*-PAA) branch chains was prepared by reversible addition-fragmentation chain transfer (RAFT) polymerization in DMF. The chain transfer agent was obtained by modification of chitosan with 3-benzylsulfanyl thiocarbonylsulfanyl propionic acid (BPATT) with 68% the degree of substitute. The graft polymerizations possessed controlled/living characteristics. The behavior of the graft copolymer in aqueous solution was investigated by dynamic light scattering, transmission electron microscopy, and UV-visible spectrophotometer. *N*-Phthaloylchitosan-*graft*-(poly(*N*-isopropylacrylamide)-*block*-poly(acrylic acid)) copolymer (*N*-phthaloylchitosan-*g*-(PNIPAAm-*b*-PAA)) could assemble to micelles in aqueous solution in range of 200–300 nm with narrow size distribution, and the hydrodynamic diameter could be controlled dependent on length of branch chains and temperature. The LCST values of micelle could be modulated from 34 to 40 °C by controlling the constitution of branch chains, pH, and concentration.

1. Introduction

Stimuli-responsive hydrogel, called smart hydrogel, exhibits the unique property of undergoing an abrupt change in volume in response to environmental changes. These smart hydrogels have future applications in intelligent systems such as switches, sensors, actuators, bioreactors, drug delivery systems, cell culture systems and so on (Miyata, 2010). Among them, pH and temperature-responsive hydrogels have been widely studied, because these two factors can be easily applied both in vivo and in vitro. For example, poly(*N*-isopropylacrylamide) (PNIPAAm) and poly(acrylic acid) (PAA) have been intensively investigated for their stimuli-responsive properties.

PNIPAAm exhibits a lower critical solution temperature (LCST) in aqueous solution and a sharp reversible phase transition at 32.8 °C in water. PAA responds to changes in pH and ionic strength by changing coil dimensions and solubility due to protonation of the carboxylate groups (Millard et al., 2006). Combining PAA and PNIPAAm can create systems responding to several external stimuli. Poly(*N*-isopropylacrylamide)-*block*-poly(acrylic acid) copolymer (PNIPAAm-*b*-PAA) was synthesized using PAA as a macromolecular chain transfer agent, which was obtained from RAFT polymerization with 1-cyanoethyl 2-pyrrolidone-1-carbodithioate as chain transfer agent, in methanol using AIBN as initiator at 60 °C (Schilli et al., 2004). Furthermore, PNIPAAm-*b*-PAA block copolymer may form micelles or other aggregates depending on the solvent, temperature, pH, block lengths and salt concentration (Schilli et al., 2004).

Chitosan is one of the most attractive materials derived from renewable resources. It shows significant pH-responsive behavior as a natural weak base with many applications in medicine, cosmetics, agriculture, biochemical separation systems, biomaterials and drug controlled release systems (Chung, Liu, & Yang, 2010; Kumar, Muzzarelli, Muzzarelli, Sashiwa, & Domb, 2004; Li, Wang, Wu, Zhang, & Hu, 2010; Muzzarelli, 2009, 2011). Graft modification is considered as a convenient and promising approach to expand the applicability of chitosan (Jayakumar, Prabaharan, Reis, & Mano, 2005). Based on the advantages and properties of chitosan

---

* Corresponding authors. Tel.: +86 571 8795 3726; fax: +86 571 8795 3726.
** Corresponding author. Tel.: +86 371 6778 1596; fax: +86 371 6776 3698.
E-mail addresses: wangzk@zju.edu.cn (Z. Wang), huql@zju.edu.cn (Q. Hu), lmy@zzu.edu.cn (M. Liu).

0144-8617/$ – see front matter. Crown Copyright © 2012 Published by Elsevier Ltd. All rights reserved.
http://dx.doi.org/10.1016/j.carbpol.2012.09.003

and PNIPAAm-*b*-PAA, graft copolymer of chitosan and PNIPAAm-*b*-PAA will possess nonlinear chemical structure and dual sensitive properties.

Great progress has been made in the field of living radical polymerization (LRP). These methods could control the synthesis of polymers with complex architectures and site-specific functionality (Semsarilar & Perrier, 2010). Living polymerization of NIPAAm has been achieved by LRP. Controlling the polymerization of AA in aqueous medium is one especial challenge due to its very high propagation rate constant in aqueous solution and rapid gel formation rate (Ladaviere, Dorr, & Claverie, 2001). Polymerization of AA in organic solvents is generally slow. In this case, PAA is usually obtained through the polymerization of acrylates and followed by hydrolysis in the presence of trifluoroacetic acid (TFA). However, chitosan is prone to degrade in the process of hydrolysis. Compared with other living polymerization techniques, reversible addition-fragmentation chain transfer (RAFT) polymerization of AA can be carried out directly without protection of carboxyl group. Hua et al. attached *S*-1-dodecyl-*S*′-(α,α'-dimethyl-α''-acetic acid) trithiocarbonate to the chitosan chain, using them for chitosan-g-PAA (Hua, Tang, Cheng, Deng, & Zhu, 2008) and chitosan-g-PNIPAAm (Tang, Hua, Cheng, Jiang, & Zhu, 2008). The molecular weight and the polydispersity index of branch chains were closed to the expected value, indicating that the polymerizations had living characters.

In this research, we first report the synthesis and properties of *N*-phthaloylchitosan-*graft*-(poly(*N*-isopropylacrylamide)-*block*-poly(acrylic acid)) copolymer (*N*-phthaloylchitosan-g-(PNIPAAm-*b*-PAA)) from the RAFT polymerization of AA and NIPAAm (Scheme 1). Chitosan was modified with 3-benzylsulfanyl thiocarbonylsulfanyl propionic acid (BPATT), an asymmetrical trithiocarbonate, to serve as macromolecular chain transfer agent. The advantage of this strategy is that the copolymer would have the excellent control of branch structure and dual responsive properties.

2. Materials and experiments

2.1. Materials

Chitosan (degree of deacetylation = 80%, viscosity-average molecular weight = 200 kDa, Aldrich) was dried in vacuum at 40 °C overnight before use. AA (AR, China National Pharmaceutical Group Corporation) was distilled under reduced pressure and used immediately. NIPAAm (97%, Aldrich) and 2,2-azobisisobutyronitrile (AIBN, 98%, Aladdin) were recrystallized twice from hexamethylene and methanol, respectively. BPATT was synthesized according to the related reference (Lai, Filla, & Shea, 2002). 1,3-Dicyclohexylcarbodiimide (DCC, 99%, Alfa Aesar) and 4-(*N*,*N*-dimethylamino) pyridine (DMAP, 99%, Alfa Aesar) were used as received. *N,N*-Dimethyl formamide (DMF) was distilled under reduced pressure from calcium hydride and stored over molecular sieves. All other reagents were of analytical grade and used without purification.

2.2. Synthesis of N-phthaloylchitosan–BPATT

N-Phthaloylated chitosan was synthesized by two steps, according to the previous literature (Kurita, Ikeda, Shimojoh, & Yang, 2007). In brief, chitosan reacted with excess *O*-pathalic anhydride in anhydrous DMF and followed by hydrolysis to obtain *N*-phthaloylchitosan. Then, the dried *N*-phthaloylchitosan (0.3 g, 1.1 mmol of C-6 hydroxyl), BPATT (0.31 g, 1.1 mmol) and DMAP (0.016 g, 0.13 mmol) were dissolved in anhydrous DMF (50 mL). After stirring for 1 h, DCC (0.23 g, 1.1 mmol) was added to the solution. The mixture was stirred for 48 h at room temperature before it was poured into ice water. The chitosan macromolecular chain transfer agent (*N*-phthaloylchitosan–BPATT) was purified by extraction with acetone and dried in vacuum at 40 °C.

^{1}H NMR (DMSO-d$_6$): δ (ppm) = 7.6–8.0 (m, $-C_6H_4-$ of *N*-phthaloyl), 7.2–7.5 (m, $-C_6H_5$ of BPATT), 4.6 ppm (s, $-CH_2-$ of benzyl), 2.8–5.2 (m, *H*-1–*H*-6 of pyranose). FTIR (KBr, cm^{-1}): 3300–3590 (ν_{O-H}), 2930 (ν_{C-H}), 1772 and 1710 (phthalimido groups), 1276 (ν_{sC-O-C}), 1138 ($\nu_{asC-O-C}$), 721 (δ_{C-H} of aromatic ring).

2.3. Polymerization of N-phthaloylchitosan-graft-poly(acrylic acid)

In a general procedure, *N*-phthaloylchitosan–BPATT (0.05 g, 0.073 mmol of trithio groups) was dissolved in dry DMF (20 mL). After dissolving completely, AIBN (0.0032 g, 0.02 mmol) and AA (1.0 g, 13.9 mmol) were added. The reaction system was removed oxygen with three freeze–pump–thaw cycles. The polymerization proceeded at 80 °C for specified time, and was terminated by immersing into liquid N_2. The *N*-phthaloylchitosan-*graft*-poly(acrylic acid) copolymer (*N*-phthaloylchitosan-*g*-PAA) was purified by pouring its DMF solution into 10-fold dichloromethane to remove residual monomer, and dried in vacuum at 40 °C to get a yellow powder.

^{1}H NMR (DMSO-d$_6$): δ (ppm) = 12.3 (s, $-COOH$), 7.8–8.0 (m, $-C_6H_4-$ of *N*-phthaloyl), 7.1–7.3 (m, $-C_6H_5$ of BPATT), 2.2 (s, $-CH-$ of PAA), 1.5 and 1.7 (d, $-CH_2-$ of PAA). FTIR (KBr, cm^{-1}): 3500–2500 (ν_{O-H}).

2.4. Polymerization of N-phthaloylchitosan-g-(PNIPAAm-b-PAA)

In brief, *N*-phthaloylchitosan-g-PAA (0.3 g, $M_{n,PAA}$ = 5335, 0.032 mmol of trithio groups) and dried DMF (15 mL) were stirred magnetically in an ampoule. After dissolving completely, NIPAAm (1.4 g, 12.4 mmol) and AIBN (0.0028 g, 0.017 mmol) were added. After degassing by three freeze–pump–thaw cycles, the reaction was continued for determined time at 60 °C. The reaction was terminated by immersing the ampoule into liquid N_2. The mixture was then purified by precipitation with diethyl ether to remove residual monomer, and dried in vacuum at 40 °C. The conversion of the monomer in solution for polymerization was determined gravimetrically after dried completely.

^{1}H NMR (DMSO-d$_6$): δ (ppm) = 12.3 (s, $-COOH$), 7.9–8.0 (m, $-C_6H_4-$ of *N*-phthaloyl), 7.1–7.4 (m, $-C_6H_5$ of BPATT and $-NH-$ of PNIPAAm), 3.8 (s, $-CH(CH_3)_2$ of PNIPAAm), 2.2 (s, $-CH-$ of PAA), 1.2–2.0 (m, $-CH_2-$ of PAA and $-CH_2-$, $-CH-$ of PNIPAAm), 1.0 (s, $-CH_3$ of PNIPAAm). FTIR (KBr, cm^{-1}): 1719 ($\nu_{C=O}$), 1645 ($\nu_{C=O}$ of amide), 1445 (δ_{C-H} of $-CH_3$).

2.5. Measurement

^{1}H NMR spectra were recorded at room temperature with a Bruker spectrometer operating at 400 MHz by using DMSO-d$_6$ as the solvent. Chemical shifts (δ) are given in ppm using tetramethylsilane (TMS) as internal reference.

FTIR spectra were recorded on Nicolet 6700 at room temperature, the samples were prepared by the squash method with KBr.

The lower critical solution temperature (LCST) of graft polymer was determined by UV-visible spectrophotometer (Shimadzu, UV-2550PC) at wavelength of 500 nm. The LCST value of the copolymer solution was defined as the temperature producing a 50% decrease in transmittance. The temperature of the sample cells was increased from 24 to 52 °C.

The hydrodynamic diameters (D_h) of the graft copolymer micelles and the polydispersity index (PDI) were determined by DLS (Delsa Nano C, Beckman Coulter) with a scattering angle of 165°

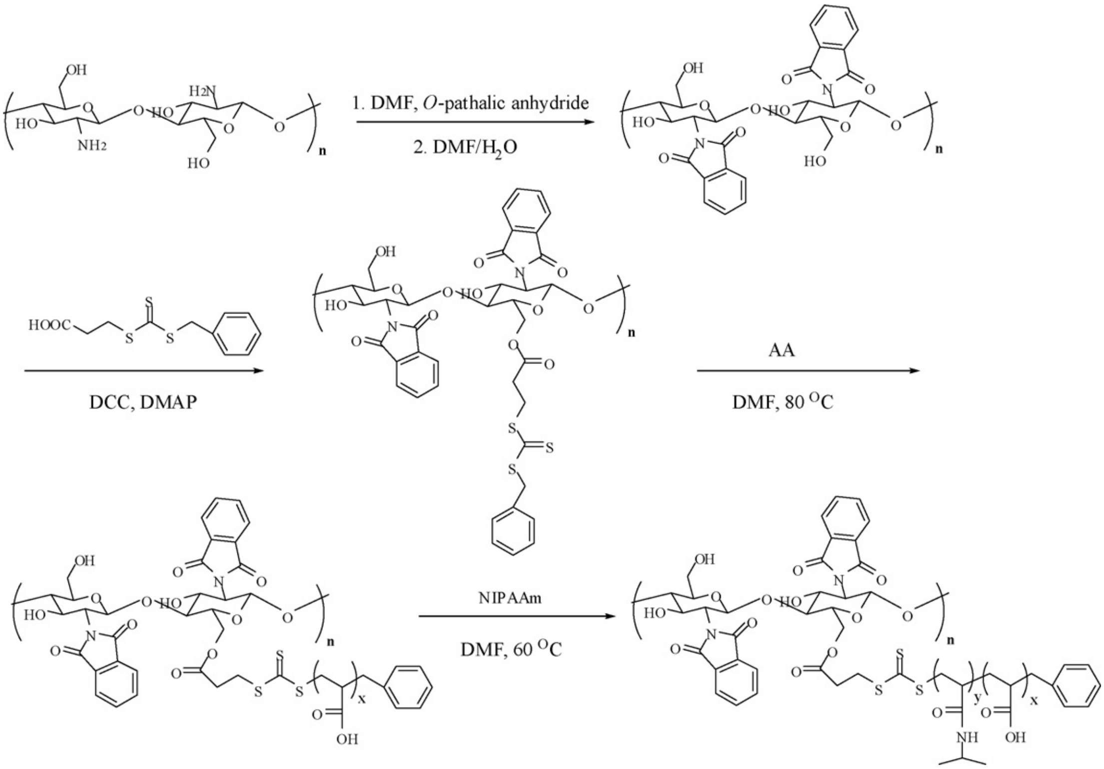

Scheme 1. Schematic synthesis of *N*-phthaloylchitosan-*g*-(PNIPAAm-*b*-PAA) using RAFT technique.

at 25 °C and 40 °C. The solutions were prepared with 0.5 mg/mL and filtered through nylon filters (pore size 0.45 μm).

TEM measurements were performed on an electron microscope (JEM-1200EX, JEOL) with an acceleration voltage of 120 kV at room temperature. Samples were prepared by placing a drop of the aqueous solution on a copper grid, which was covered with a perforated polymer film and coated with carbon on both sides. The sample film was thinned by blotting.

3. Result and discussion

In order to increase the solubility of chitosan, phthaloylation may be regarded as the most effective method. Chitosan reacted with PA resulted in partial *O*-phthaloylation, and the *O*-phthaloyl group could be removed by hydrolysis for 5 h in DMF containing 5% H_2O. The degree of substitution of phthaloyl group was determined to be 97% by elemental analysis. In this research, the chitosan macromolecular chain transfer agent was prepared through modification with BPATT. BPATT, an asymmetric trithiocarbonate, has been already used as a chain transfer agent (CTA) for preparation of well-defined, functional polymers containing AA, NIPAAm and butyl acetate (BA) (Moad, Rizzardo, & Thang, 2006). In addition, BPATT has the ability to generate different architectures, such as hyper branch or star polymers, via the carboxylic group. Fig. 1b shows the ^{1}H NMR spectrum of *N*-phthaloylchitosan–BPATT. The new characteristic peaks at 7.2–7.4 ppm, 4.6 ppm were attributed to phenmethyl protons in BPATT. FTIR spectrum (Fig. 2c) also confirms the structure of *N*-phthaloylchitosan–BPATT. The FTIR spectrum of *N*-phthaloylchitosan–BPATT was no significant difference than that of *N*-phthaloylchitosan, probably attributed to the absorption overlap of the trithiocarbonate (1062 cm^{-1}) and chitosan (1077 cm^{-1}). The characteristic peaks at 1276 cm^{-1} and 1138 cm^{-1} were assigned to the asymmetrical stretching vibration and symmetrical stretching vibration of ester group. These spectra analysis confirmed the successful synthesis of *N*-phthaloylchitosan–BPATT. After the esterification between *N*-phthaloylchitosan and BPATT, the degree of substitution was 68% determined by ^{1}H NMR spectrum, which meant the concentration of trithio group was 1.46 mmol/g in *N*-phthaloylchitosan–BPATT. Due to steric hindrance, it was inferred that the esterification should be preceded at C-6 position.

AA was polymerized in present of *N*-phthaloylchitosan–BPATT and AIBN. The polymerization was carried out in 20 mL DMF, in which the RAFT agent was almost soluble. The graft copolymer

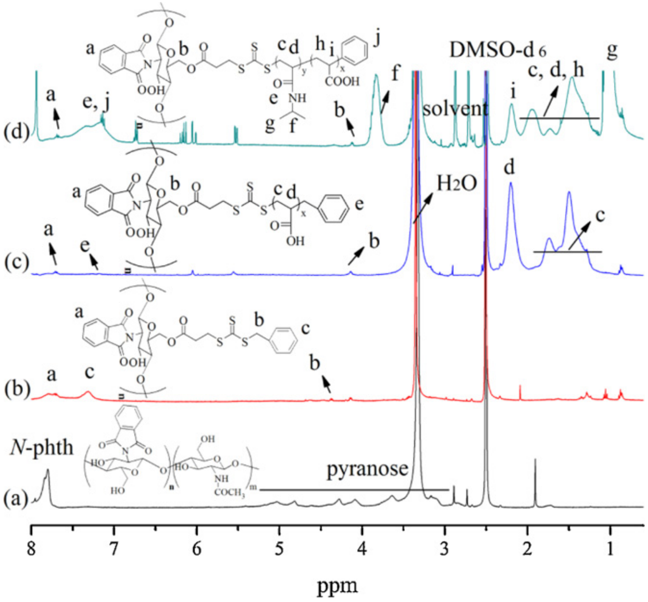

Fig. 1. ^{1}H NMR spectra of *N*-phthaloylchitosan (a), *N*-phthaloylchitosan–BPATT (b), *N*-phthaloylchitosan-*g*-PAA (c, *t* = 2.5 h) and *N*-phthaloylchitosan-*g*-(PNIPAAm-*b*-PAA) (d, *t* = 72 h).

Table 1
The results of the RAFT polymerization of AA in DMF.

$[M]_0/[CTA]_0$	$[M]_0$ (mol/L)	Time (h)	Conv.[a] (%)	$M_{n,theor}$ [b] (g/mol)	$M_{n,exp}$ [c] (g/mol)
190	0.7	1	1.5	487	887
190	0.7	1.5	7.2	1267	1737
190	0.7	2	19.4	2936	3225
190	0.7	2.5	34.5	5002	5335
190	0.7	3	62.7	8859	9094
190	0.7	4	73.1	10,282	12,585

[a] Monomer conversion was calculated according to the equation, Conv. (%) = $W_P - W_0)/W_M \times 100$.
[b] The theoretical number-average molecular weight was calculated according to the equation, $M_{n,theor} = M_M \times \text{Conv} \times [M]_0/[CTA]_0 + M_{CTA}$.
[c] The experimental number-average molecular weight was calculated by ^{1}H NMR spectroscopy in DMSO-d_6.

structures were characterized by ^{1}H NMR and FTIR spectra. Except for the peaks of *N*-phthaloylchitosan, the characteristic peaks of PAA were detected at 12.3 ppm, 2.2 ppm and 1.2–1.8 ppm, which were assigned to protons of carboxyl group, methylene and methyl, respectively (Fig. 1c). Compared with the FTIR spectrum of *N*-phthaloylchitosan–BPATT, the absorption band between 2500 and 3500 cm^{-1} became wider indicating the formation of carboxyl group, and the characteristic bond at 1720 cm^{-1} (stretching of $C{=}O$) enhanced in case of *N*-phthaloylchitosan-*g*-PAA. The results indicated the formation of *N*-phthaloylchitosan-*g*-PAA using the RAFT technique. The results of polymerization are summarily listed in Table 1. The kinetic data given in Table 1 clearly indicated that *N*-phthaloylchitosan–BPATT could allow an excellent control of AA polymerization in DMF. With the BAPTT/AIBN ratio of 3.6 and the AA/BAPTT ratio of 190, the first-order time-conversion displayed an induction period of about 1 h. After the introduction period, the RAFT equilibrium was established, and the reaction was dependent on reaction time during the major part of polymerization. It was obvious that the number-average molecular weight increased linearly with polymerization time. The values of experiment molecular weight were slightly larger than those of the theoretical, which may be associated with the experimental error of the Conv. and the difference of the methods of calculation. All the evidences proved that the RAFT polymerization was well controlled in the process.

RAFT technique is considered as one of the most versatile methods for synthesis well defined complex architectures, such as block copolymer. In RAFT polymerization, the order of constructing the blocks of a block copolymer should be very important (Chong et al., 2003; Moad, Rizzardo, & Thang, 2009). The propagating radical for the first formed block must be a good homolytic leaving group with respect to that of the second block. *N*-Phthaloylchitosan-*g*-(PNIPAAm-*b*-PAA) was synthesized using *N*-phthaloylchitosan-*g*-PAA containing trithiocarbonate groups as a macromolecular CTA, which was at a ratio of 1/74 or 1/126 compared to PAA block length. The polymerization of NIPAAm usually carried out in pure water. Because *N*-phthaloylchitosan-*g*-PAA could aggregate in pure water, the aggregation leads to a full collapse of the block copolymers which results in a loss of control (Millard et al., 2010). To avoid this loss, the polymerization of NIPAAm was still carried out in DMF in our study. The structure of finally graft copolymer was also confirmed by spectral analysis. In ^{1}H NMR spectrum (Fig. 2d), several new peaks at 1.1 ppm, 1.2–1.6 ppm, 2.3 ppm, 3.8 ppm and 7.0–7.5 ppm were assigned to the characteristic resonances of PNIPAAm block. Fig. 3e and f shows the FTIR spectra of *N*-phthaloylchitosan-*g*-(PNIPAAm-*b*-PAA) obtained under special polymerization time. The spectrum of *N*-phthaloylchitosan-*g*-(PNIPAAm-*b*-PAA) obtained for 24 h was similar to that of *N*-phthaloylchitosan-*g*-PAA, because the content of PNIPAAm was too low to be detected. Minko et al. discussed the theoretical background of the radical polymerization initiated from a solid substrate in which the initiator was attached to the surface (Minko, Gafijchuk, Sidorenko, & Voronov, 1999). The subsequent grafting of new chains could not start until the initiator stretched to the maximum possible surface. That may be used to explain why the content of PNIPAAm was so low after 24 h. With the polymerization time increase, the characteristic peaks at 1645 cm^{-1} (stretching of $C{=}O$ in amide) and 1454 cm^{-1} (bending of $C{-}H$ in methyl) were appeared in Fig. 2e, and the absorption intensity of $C{-}H$ stretching was greatly enhanced. These results further demonstrated the successful in chain extension experiments of PNIPAAm. To further demonstrate the functionality of the residual trithiocarbonate and

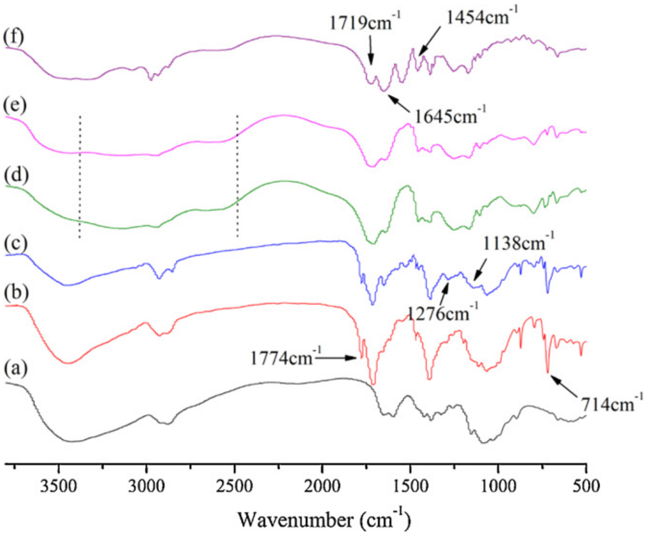

Fig. 2. FTIR spectra of chitosan (a), *N*-phthaloylchitosan (b), *N*-phthaloylchitosan–BPATT (c), *N*-phthaloylchitosan-*g*-PAA (d, *t* = 2.5 h), *N*-phthaloylchitosan-*g*-(PNIPAAm-*b*-PAA) (e, *t* = 24 h) and *N*-phthaloylchitosan-*g*-(PNIPAAm-*b*-PAA) (f, *t* = 72 h).

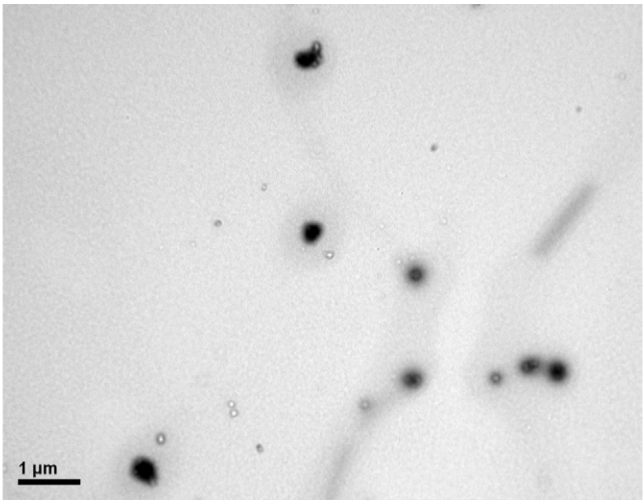

Fig. 3. TEM image for *N*-phthaloylchitosan-*g*-(PNIPAAm-*b*-PAA) cast from aqueous solution.

Table 2
Block extension of PNIPAAm by RAFT polymerization in DMF.

Sample	Monomer	$[M]_0/[CTA]_0$	$[M]_0$ (mol/L)	Time (h)	Conv.[b] (%)	$M_{n,theor}$ [c] (g/mol)	$M_{n,exp}$ [d] (g/mol)	DP_{AA}/DP_{NIPAAm}
A[a]	AA	190	0.7	2.5	34.5	5002	5335	0
B	NIPAAm	243	0.62	24	1.27	348	393	21.3
C	NIPAAm	208	0.53	48	19.9	4673	4967	1.68
D	NIPAAm	217	0.53	72	39.3	9631	9879	0.85
E[a]	AA	190	0.7	3	62.7	8859	9094	0
F	NIPAAm	302	0.53	72	39.4	13,456	16,278	0.87

[a] PAA precursor was synthesized by RAFT in DMF with *N*-phthaloylchitosan–BPATT as macro-CTA.
[b] Monomer conversion was calculated according to the equation, Conv. (%) = $(W_P - W_0)/W_M \times 100$.
[c] The theoretical number-average molecular weight of PNIPAAm was calculated according to the equation, $M_{n,theor} = M_M \times \text{Conv.} \times [M]_0/[CTA]_0$.
[d] The experimental number-average molecular weight was calculated by ^{1}H NMR spectroscopy in DMSO-d_6.

the controlled nature in the chain extension of the PNIPAAm, the experimental data are detailed in Table 2. The chain extension of the PNIPAAm was nearly quantitative with the polymerization time. Such evidence suggested that the macromolecular chain transfer agent was available for subsequent chain extension and stable during the polymerization.

In this research, the polydispersity of chitosan was unknown, so the polydispersity of branch chain cannot be analyzed through size exclusion chromatography. Barner reported that the RAFT approach offers a key advantage in that the growing tethered chains generated on the surface were in a dynamic equilibrium with untethered chains in the solution phase (Barner, Zwaneveld, Perera, Pham, & Davis, 2002). However, there was little homo-PAA found in our experiment because the high ratio of $[CTA]_0/[I]_0$ can prevent the number of dead chains from exceeding 5% (Smith, Xu, & McCormick, 2010), and the homo-polymer cannot be separated from the system through exhaustive extraction mentioned by Hua (Hua et al., 2008), because portion of graft copolymer could dissolve in the process of separation through exhaustive extraction with hot water and ethanol. It was reported that the morphologies of graft copolymer were associated with the polydispersity of the copolymer (Shen, Yu, & Huang, 2005). Fig. 3 shows the corresponding TEM image at 25 °C. The symmetric spheres with 200–300 nm diameters and shell-corona structure were clearly seen in the image. Micelles were formed in aqueous solution with chitosan forming the micellar core and PNIPAAm-*b*-PAA forming the corona. To further investigate the structures of micelles in solution, DLS measurements were performed on graft copolymer aqueous solution at 25 °C and 40 °C (Fig. 4). The size distribution was very narrow, which can be associated with the "well-defined" branch chains. It is found that the hydrodynamic diameter (D_h) of the graft copolymer in water increased with the branch side chains. This also offers further evidence of the structure of micelles. Comparing the results at 25 °C and 40 °C, micelle had the smaller D_h and the narrower size distribution at high temperature. This should attribute to the block of PNIPAAm collapsed into the coils at 40 °C, resulted D_h decreasing.

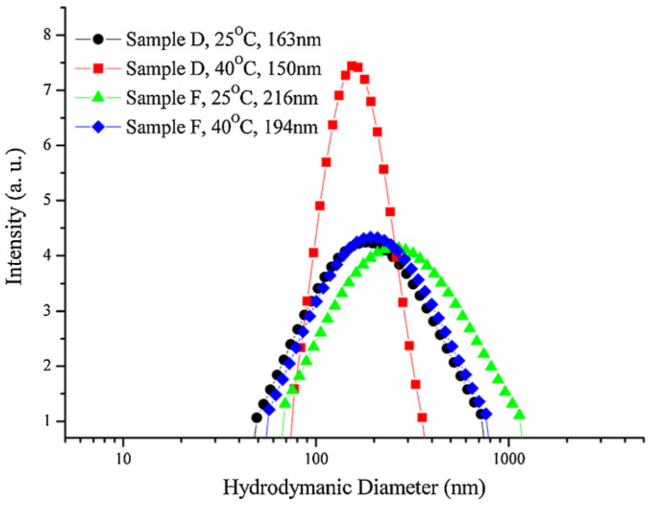

Fig. 4. DLS analysis in water at 25 °C and 40 °C.

In order to evaluate the thermo sensitive behavior of *N*-phthaloylchitosan-*g*-(PNIPAAm-*b*-PAA), Fig. 5 shows the transmittance curves of solution of *N*-phthaloylchitosan-*g*-(PNIPAAm-*b*-PAA) at different temperatures and pHs. For all the samples, a decrease of the transmittance was observed with the increasing temperature. The LCST value of the copolymer solution was defined as the temperature producing a 50% decrease in transmittance. At pH 7.0, the LSCT of sample D and sample F solutions with the 0.4 mg/mL concentration were 37.2 °C and 39 °C and the LCST of sample D solutions with the 0.8 mg/mL concentration was 38.7 °C. Generally, the PNIPAAm homopolymer exhibits a sharp reversible phase transition at 32–34 °C in water. The LCST of PNIPAAm can be effectively controlled by incorporating hydrophilic or hydrophobic units (Zhang, Srivastava, & Misra, 2007). The LCST values of all

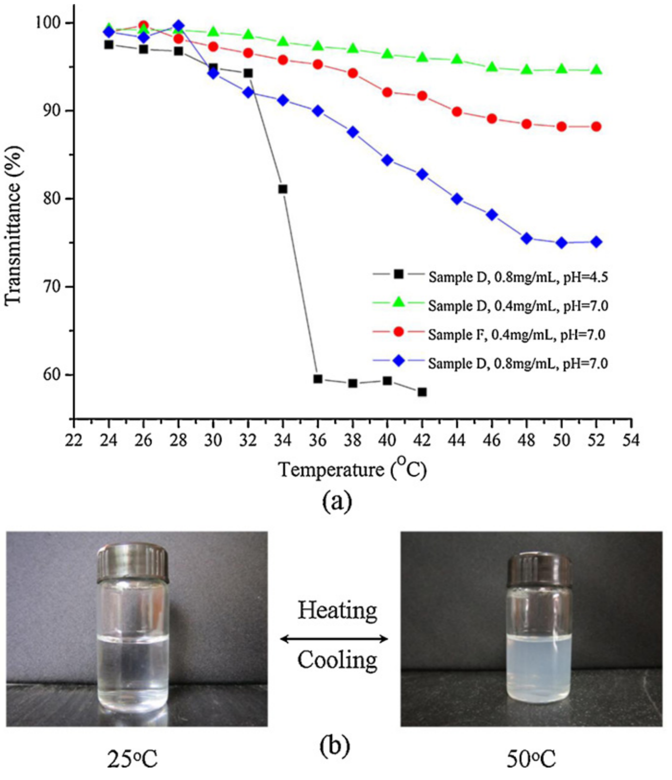

Fig. 5. Transmittance of aqueous solutions of graft polymers as a function of temperature (a) and optical photograph of sample D aqueous solution (0.8 mg/mL, pH = 7.0) at 25 °C and 50 °C (b).

N-phthaloylchitosan-*g*-(PNIPAAm-*b*-PAA) were higher than that of PNIPAAm. This phenomenon was considered to the connection of PNIPAAm block with hydrophilic PAA block. With the M_n of PNIPAAm and PAA blocks increasing, the LCST value was ascended. The phenomenon was easy to understand with the interaction between two blocks, which was increased with the ratio of hydrophilic PAA to PNIPAAm increasing. Interestingly, it was found that the concentration also affected the LCST. The sample D with the 0.8 mg/mL concentration was 38.7 °C, higher than that of 0.4 mg/mL. In addition, the graft copolymer showed a wide phase transition with a temperature range of about 18 °C, not a sharp phase transition like that of PNIPAAm. The difference may arise from the different aggregation structures. On the one hand, the PNIPAAm chain in homo-polymer could move freely, comparatively, PNIPAAm in *N*-phthaloylchitosan-*g*-(PNIPAAm-*b*-PAA) was tethered to the core of chitosan and PAA block. When the temperature changed, the movement of PNIPAAm blocks was constrained than the free PNIPAAm chains. On the other hand, this phenomenon also ascribed to the effect of solubilization of PAA blocks, which was confirmed through the experiment. At pH 4.5, transmittance of sample D with the 0.8 mg/mL concentration decreased rapidly when the temperature was raised above LCST, 34.2 °C, indicating forming large aggregates easily due to insoluble of PAA blocks.

4. Conclusion

In this research, *N*-phthaloylchitosan-*g*-(PNIPAAm-*b*-PAA) was obtained by RAFT polymerization. *N*-Phthaloylchitosan was modified with BPATT to serve as macro RAFT agent, and then the graft polymerizations of AA and NIPAAm were successively performed in DMF. The controlled/living characteristics were proven for the polymerizations. ^{1}H NMR and FTIR spectra demonstrate the successful synthesis of the graft copolymer. *N*-phthaloylchitosan-*g*-(PNIPAAm-*b*-PAA) could assemble to micelles in aqueous solution in range of 200–300 nm with narrow size distribution, and the hydrodynamic diameter could be controlled dependent on length of branch chains and temperature. Hydrogen bonding in PNIPAAm-*b*-PAA branch chains influenced strongly their behavior in solution. Transmittance measurements indicated LCST of the graft copolymer aqueous solution was a little higher than that of PNIPAAm solution at pH 7.0. The graft copolymer showed a wide phase transition at pH 7.0, but exhibited a sharp reversible phase transition at pH 4.0.

Acknowledgments

This work was financially supported by National Natural Science Foundation of China (Nos. 21104067 and 21274127), Key Basic Research Development Plan (973) of China (Nos. 2009CB930104 and 2011CB606203).

References

Barner, L., Zwaneveld, N., Perera, S., Pham, Y., & Davis, T. P. (2002). Reversible addition-fragmentation chain-transfer graft polymerization of styrene: Solid phases for organic and peptide synthesis. *Journal of Polymer Science Part A: Polymer Chemistry*, *40*, 4180–4192.

Chong, Y. K., Krstina, J., Le, T. P. T., Moad, G., Postma, A., Rizzardo, E., et al. (2003). Thiocarbonylthio compounds [S=C(Ph)S—R] in free radical polymerization with reversible addition-fragmentation chain transfer (RAFT polymerization). Role of the free-radical leaving group (R). *Macromolecules*, *36*, 2256–2272.

Chung, T. W., Liu, D. Z., & Yang, J. S. (2010). Effects of interpenetration of thermo-sensitive gels by crosslinking of chitosan on nasal delivery of insulin: In vitro characterization and in vivo study. *Carbohydrate Polymers*, *82*, 316–322.

Hua, D. B., Tang, J., Cheng, J. X., Deng, W. C., & Zhu, M. L. (2008). A novel method of controlled grafting modification of chitosan via RAFT polymerization using chitosan-RAFT agent. *Carbohydrate Polymers*, *73*, 98–104.

Jayakumar, R., Prabaharan, M., Reis, R. L., & Mano, J. F. (2005). Graft copolymerized chitosan—Present status and applications. *Carbohydrate Polymers*, *62*, 142–158.

Kumar, M., Muzzarelli, R. A. A., Muzzarelli, C., Sashiwa, H., & Domb, A. J. (2004). Chitosan chemistry and pharmaceutical perspectives. *Chemical Reviews*, *104*, 6017–6084.

Kurita, K., Ikeda, H., Shimojoh, M., & Yang, J. (2007). N-phthaloylated chitosan as an essential precursor for controlled chemical modifications of chitosan: Synthesis and evaluation. *Polymer Journal*, *39*, 945–952.

Ladaviere, C., Dorr, N., & Claverie, J. P. (2001). Controlled radical polymerization of acrylic acid in protic media. *Macromolecules*, *34*, 5370–5372.

Lai, J. T., Filla, D., & Shea, R. (2002). Functional polymers from novel carboxyl-terminated trithiocarbonates as highly efficient RAFT agents. *Macromolecules*, *35*, 6754–6756.

Li, Y. Z., Wang, Y. X., Wu, D., Zhang, K., & Hu, Q. L. (2010). A facile approach to construct three-dimensional oriented chitosan scaffolds with in situ precipitation method. *Carbohydrate Polymers*, *80*, 408–412.

Millard, P. E., Barner, L., Reinhardt, J., Buchmeiser, M. R., Barner-Kowollik, C., & Muller, A. H. E. (2010). Synthesis of water-soluble homo- and block-copolymers by RAFT polymerization under gamma-irradiation in aqueous media. *Polymer*, *51*, 4319–4328.

Millard, P. E., Barner, L., Stenzel, M. H., Davis, T. P., Barner-Kowollik, C., & Muller, A. H. E. (2006). RAFT polymerization of N-isopropylacrylamide and acrylic acid under gamma-irradiation in aqueous media. *Macromolecular Rapid Communications*, *27*, 821–828.

Minko, S., Gafijchuk, G., Sidorenko, A., & Voronov, S. (1999). Radical polymerization initiated from a solid substrate. 1. Theoretical background. *Macromolecules*, *32*, 4525–4531.

Miyata, T. (2010). Preparation of smart soft materials using molecular complexes. *Polymer Journal*, *42*, 277–289.

Moad, G., Rizzardo, E., & Thang, S. H. (2006). Living radical polymerization by the RAFT process—A first update. *Australian Journal of Chemistry*, *59*, 669–692.

Moad, G., Rizzardo, E., & Thang, S. H. (2009). Living radical polymerization by the RAFT process—A second update. *Australian Journal of Chemistry*, *62*, 1402–1472.

Muzzarelli, R. A. A. (2009). Chitins and chitosans for the repair of wounded skin, nerve, cartilage and bone. *Carbohydrate Polymers*, *76*, 167–182.

Muzzarelli, R. A. A. (2011). Potential of chitin/chitosan-bearing materials for uranium recovery: An interdisciplinary review. *Carbohydrate Polymers*, *84*, 54–63.

Schilli, C. M., Zhang, M. F., Rizzardo, E., Thang, S. H., Chong, Y. K., Edwards, K., et al. (2004). A new double-responsive block copolymer synthesized via RAFT polymerization: Poly(N-isopropylacrylamide)-block-poly(acrylic acid). *Macromolecules*, *37*, 7861–7866.

Semsarilar, M., & Perrier, S. (2010). 'Green' reversible addition-fragmentation chain-transfer (RAFT) polymerization. *Nature Chemistry*, *2*, 811–820.

Shen, D. W., Yu, H., & Huang, Y. (2005). Densely grafting copolymers of ethyl cellulose through atom transfer radical polymerization. *Journal of Polymer Science Part A: Polymer Chemistry*, *43*, 4099–4108.

Smith, A. E., Xu, X. W., & McCormick, C. L. (2010). Stimuli-responsive amphiphilic (co)polymers via RAFT polymerization. *Progress in Polymer Science*, *35*, 45–93.

Tang, J., Hua, D. B., Cheng, J. X., Jiang, J., & Zhu, X. L. (2008). Synthesis and properties of temperature-responsive chitosan by controlled free radical polymerization with chitosan-RAFT agent. *International Journal of Biological Macromolecules*, *43*, 383–389.

Zhang, J., Srivastava, R., & Misra, R. (2007). Core–shell magnetite nanoparticles surface encapsulated with smart stimuli-responsive polymer: Synthesis, characterization, and LCST of viable drug-targeting delivery system. *Langmuir*, *23*, 6342–6351.